

Exclusive production of $f_1(1285)$ meson in proton-(anti)proton collisions

P. Lebedowicz

*Institute of Nuclear Physics Polish Academy of Sciences,
Radzikowskiego 152, PL-31342 Kraków, Poland.
e-mail: Piotr.Lebedowicz@ifj.edu.pl*

Received 15 December 2021; accepted 20 January 2022

We discuss the exclusive production of axial-vector $f_1(1285)$ meson via the vector-vector fusion mechanism at energies relevant for the HADES and PANDA experiments at FAIR. Total and differential cross sections are given. The possibility of a measurement by HADES at $\sqrt{s} = 3.46$ GeV is presented and discussed. The decay channel $f_1 \rightarrow \pi^+ \pi^- \eta (\rightarrow \pi^+ \pi^- \pi^0)$ seems particularly promising for this purpose.

Keywords: Exclusive reactions; axial-vector meson; $f_1(1285)$; proton-proton and proton-antiproton collisions; HADES; PANDA; FAIR.

DOI: <https://doi.org/10.31349/SuplRevMexFis.3.0308050>

1. Introduction

We present a new study of the exclusive production of axial-vector $f_1(1285)$ meson ($J^{PC} = 1^{++}$) at energies relevant for the HADES (pp) and PANDA ($p\bar{p}$) experiments; see *e.g.* [1, 2]. The PANDA experiment (antiProton ANnihilations at DArmstadt) will be one of the key experiments at the Facility for Antiproton and Ion Research (FAIR). This presentation summarises some of the key results of [3] to which we refer the reader for further details. We assumed that at energies close to the threshold the $\omega\omega \rightarrow f_1(1285)$ and $\rho^0\rho^0 \rightarrow f_1(1285)$ fusion processes (Fig. 1) are dominant. Future experiments (HADES, PANDA) will provide new information on the couplings of $\omega\omega \rightarrow f_1$ and $\rho^0\rho^0 \rightarrow f_1$. From such experiments we will learn more on the nature of the $f_1(1285)$ meson, for instance, is it a $q\bar{q}$ state or $\bar{K}K^*$ molecule?.

At higher energies (RHIC, LHC) the pomeron-pomeron fusion mechanism ($\mathbb{P}\mathbb{P} \rightarrow f_1$) is expected to be dominant. In Ref. [4] the $pp \rightarrow pp f_1(1285)$ and $pp \rightarrow pp f_1(1420)$ reactions were considered in the tensor-pomeron approach [6]. A good description of the WA102 data at $\sqrt{s} = 29.1$ GeV was obtained. It was emphasized in Appendix D of [4] that at the lower WA102 energy $\sqrt{s} = 12.7$ GeV the reggeized-vector-meson or reggeon exchange contributions should be taken into account. This studies could be extended by the COMPASS experiment where presumably one could study the influence of reggeon exchanges. A study of central exclusive production (CEP) of the axial-vector mesons could shed more light on the coupling of two reggeons/pomerons

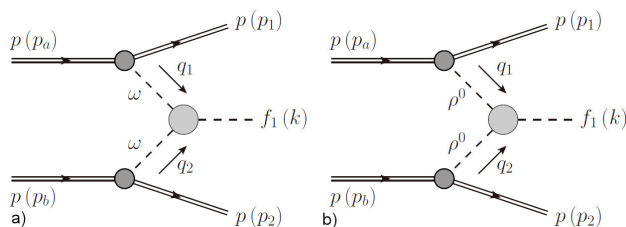


FIGURE 1. Diagrams for the $pp \rightarrow pp f_1$ reaction via the $\omega\omega$ - and $\rho\rho$ -fusion processes.

to the f_1 . In particular, the theoretical calculation of $\mathbb{P}\mathbb{P}f_1$ coupling is a challenging problem of nonperturbative QCD. The four-pion decay channel seems well suited to measure the $f_1(1285)$ meson at the LHC. The measurement of 4π CEP has already been initiated by the ATLAS Collaboration [5].

2. Formalism sketch

We discuss exclusive production of $f_1(1285)$ resonance in proton-(anti)proton collisions close to the threshold: $p(p_a, \lambda_a) + p(p_b, \lambda_b) \rightarrow p(p_1, \lambda_1) + f_1(k, \lambda) + p(p_2, \lambda_2)$. Here $p_{a,b}$, $p_{1,2}$ and $\lambda_{a,b}$, $\lambda_{1,2} = \pm 1/2$ denote the four-momenta and helicities of the protons, and k and $\lambda = 0, \pm 1$ denote the four-momentum and helicity of the f_1 meson.

The amplitude for $pp \rightarrow pp f_1(1285)$ includes two terms

$$\mathcal{M}_{pp \rightarrow pp f_1} = \mathcal{M}_{pp \rightarrow pp f_1}^{(\omega\omega \text{ fusion})} + \mathcal{M}_{pp \rightarrow pp f_1}^{(\rho\rho \text{ fusion})}. \quad (1)$$

The VV -fusion amplitude ($VV = \rho^0\rho^0$ or $\omega\omega$) reads

$$\begin{aligned} \mathcal{M}_{\lambda_a \lambda_b \rightarrow \lambda_1 \lambda_2 \lambda_{f_1}}^{(VV \text{ fusion})} &= (-i) (\epsilon^\alpha(\lambda_{f_1}))^* \\ &\times \bar{u}(p_1, \lambda_1) i\Gamma_{\mu_1}^{(Vpp)}(p_1, p_a) u(p_a, \lambda_a) \\ &\times i\tilde{\Delta}^{(V)\mu_1\nu_1}(s_1, t_1) i\Gamma_{\nu_1\nu_2\alpha}^{(VVf_1)}(q_1, q_2) \\ &\times i\tilde{\Delta}^{(V)\nu_2\mu_2}(s_2, t_2) \\ &\times \bar{u}(p_2, \lambda_2) i\Gamma_{\mu_2}^{(Vpp)}(p_2, p_b) u(p_b, \lambda_b). \end{aligned} \quad (2)$$

The kinematic variables are

$$\begin{aligned} q_1 &= p_a - p_1, \quad q_2 = p_b - p_2, \quad k = q_1 + q_2, \\ t_1 &= q_1^2, t_2 = q_2^2, \quad m_{f_1}^2 = k^2, \\ s &= (p_a + p_b)^2 = (p_1 + p_2 + k)^2, \\ s_1 &= (p_1 + k)^2, \quad s_2 = (p_2 + k)^2. \end{aligned} \quad (3)$$

In Eq. (2) $\epsilon_\alpha(\lambda)$ is the polarisation vector of the f_1 meson, $\Gamma_\mu^{(Vpp)}$ and $\Gamma_{\nu_1\nu_2\alpha}^{(VVf_1)}$ are the Vpp and VVf_1 vertex functions, respectively (see [3] for details of all these quantities):

$$i\Gamma_{\mu}^{(Vpp)}(p', p) = -i\Gamma_{\mu}^{(V\bar{p}\bar{p})}(p', p) = -ig_{Vpp} F_{VNN}(t) \left[\gamma_{\mu} - i \frac{\kappa_V}{2m_p} \sigma_{\mu\nu} (p - p')^{\nu} \right], \quad (4)$$

$$i\Gamma_{\mu\nu\alpha}^{(VVf_1)}(q_1, q_2) |_{\text{bare}} = \frac{2g_{VVf_1}}{M_0^4} \left[(q_1 - q_2)^{\rho} (q_1 - q_2)^{\sigma} \varepsilon_{\lambda\sigma\alpha\beta} k^{\beta} (q_{1\kappa} \delta_{\mu}^{\lambda} - q_{1\lambda} g_{\kappa\mu}) (q_2^{\kappa} g_{\rho\nu} - q_{2\rho} \delta_{\nu}^{\kappa}) + (q_1 \leftrightarrow q_2, \mu \leftrightarrow \nu) \right], \quad (5)$$

$$M_0 = 1 \text{ GeV}.$$

For the V -(anti)proton coupling constants in Eq. (4) we use:

$$g_{ppp} = 3.0, \quad \kappa_{\rho} = 6.1, \quad g_{\omega pp} = 9.0, \quad \kappa_{\omega} = 0. \quad (6)$$

For the form factor $F_{VNN}(t)$, describing the t -dependence of the VNN coupling, we take

$$F_{VNN}(t) = \frac{\Lambda_{VNN}^2 - m_V^2}{\Lambda_{VNN}^2 - t}. \quad (7)$$

The VVf_1 vertex coupling (5) is derived from an effective coupling Lagrangian [3, 4] by considering the on shell process of two real vector particles V fusing to give an f_1 meson. The angular momentum analysis of such reactions was made in Ref. [7]. A convenient coupling Lagrangian, corresponding to $(l, S) = (2, 2)$, with orbital angular momentum l and total spin S , is given by (2.6) of [3]; see also Appendix D of [4]. In Eq. (5) the label ‘‘bare’’ means that the VVf_1 vertex is derived from the corresponding coupling Lagrangian without a form-factor function. Thus, for realistic applications, we should multiply the VVf_1 vertex by the form factor:

$$F_{VVf_1}(q_1^2, q_2^2, k^2) = \tilde{F}_V(q_1^2) \tilde{F}_V(q_2^2) F_{f_1}(k^2). \quad (8)$$

We have $F_{VVf_1}(m_V^2, m_V^2, m_V^2) = 1$. We make the assumption that $\tilde{F}_V(t)$ is parametrized as

$$\tilde{F}_V(q^2) = \frac{\Lambda_V^4}{\Lambda_V^4 + (q^2 - m_V^2)^2}, \quad (9)$$

where the cutoff parameter Λ_V , taken to be the same for both ρ^0 and ω , is a free parameter.

The standard form of the vector-meson propagator is given in (3.2) of [6]. For small values of s_i and $|t_i|$ ($i = 1, 2$) the simplest form of the transverse function, $\Delta_T^{(V)}(t) = (t - m_V^2)^{-1}$, is adequate. For larger s_i we must take into account reggeization $\Delta_T^{(V)}(t_i) \rightarrow \tilde{\Delta}_T^{(V)}(s_i, t_i)$ (see [3]),

$$\tilde{\Delta}_T^{(V)}(s_i, t_i) = \Delta_T^{(V)}(t_i) \left(\exp(i\phi(s_i)) \frac{s_i}{s_{\text{thr}}} \right)^{\alpha_V(t_i) - 1} \quad (10)$$

and $\phi(s_i) = (\pi/2) \exp([s_{\text{thr}} - s_i]/s_{\text{thr}}) - (\pi/2)$ with $s_{\text{thr}} = (m_p + m_{f_1})^2$. We use the linear form for the vector-meson Regge trajectories $\alpha_V(t) = \alpha_V(0) + \alpha'_V t$, $\alpha_V(0) = 0.5$, $\alpha'_V = 0.9 \text{ GeV}^{-2}$.

The $g_{\rho\rho f_1}$ coupling constant in Eq. (5) has been extracted from the decay rate of $f_1(1285) \rightarrow \rho^0 \gamma$ using the vector-meson-dominance (VMD) ansatz. We assumed $g_{\omega\omega f_1} = g_{\rho\rho f_1}$ based on arguments from the naive quark model and VMD. Then, we have fixed the cutoff parameters in the form factors and the corresponding coupling constants $|g_{VVf_1}|$ by fits to the CLAS experimental data for the process $\gamma p \rightarrow f_1(1285)p \rightarrow (\eta\pi^+\pi^-)p$ [8]; see Appendices B and C of [3]. There, the reggeized ρ - and ω -exchange contributions play a crucial role in describing the forward-peaked angular distributions, especially at higher energies, $W_{\gamma p} > 2.55 \text{ GeV}$. The form of reggeization used in the model, affects both, the size of the cross section and the t -dependence of the V exchanges; see the right panels of Figs. (4) and (15) of [3].

3. Selected results

In Fig. 2 we show some examples of the results for the $pp \rightarrow pp f_1(1285)$ reaction taken from [3]. Figure 2a) shows integrated cross sections for the VV -fusion mechanism as a function of collision energy \sqrt{s} . The results for three sets of parameters (C7), (C9) and (C10) are shown; see Appendix C of [3]. The result of diffractive pomeron-pomeron fusion mechanism is also shown for comparison (see the red dotted line). The VV -fusion cross section rises from the threshold $\sqrt{s} = 2m_p + m_{f_1}$ to $\sqrt{s} \approx 5 \text{ GeV}$ (PANDA energy range), then it begins to decrease due to the reggeization effect. We note that in our procedure of extracting the model parameters (from the CLAS data on $\gamma p \rightarrow f_1(1285)p$) the dominant sensitivity of the results is on g_{VVf_1} coupling constant, not on the form-factor cutoff parameters.

The distributions in $\cos \theta_M$, where θ_M is the angle between \mathbf{k} and \mathbf{p}_α in the c.m. frame, for $\sqrt{s} = 3.46 \text{ GeV}$ and

$\sqrt{s} = 5.0$ GeV have a different shape. This is illustrated in Figs. 2b) and c). The contributions for the $\omega\omega$ - and $\rho\rho$ -fusion processes separately, their coherent sum (total), and the interference term are shown. The $\omega\omega$ and $\rho\rho$ terms have different kinematic dependences. With increasing energy \sqrt{s} the averages of $|t_1|$ and $|t_2|$ decrease, damping by form factors, hence the $\omega\omega$ contribution becomes more important. However, for large values of $|t_1|$ and $|t_2|$, in spite of $g_{\rho pp} < g_{\omega pp}$ (6), the spin-flip term of the ρ^0 -proton coupling is important.

Now we discuss the reaction $pp \rightarrow pp\pi^+\pi^-\eta$ ($\rightarrow \pi^+\pi^-\pi^0$) for $\sqrt{s} = 3.46$ GeV ($E_{\text{kin}} = 4.5$ GeV). The simulations of this reaction were performed with PLUTO [9]. The four charged pions can be reconstructed in the HADES detector and the neutral pion from the η decay can be reconstructed via missing mass technique or via two photon decay; see Sec. IV of [3]. In Table I we have collected the cross sections used in the simulations. For the $VV \rightarrow f_1(1285)$ production cross section we have assumed $\sigma_{f_1} = 150$ nb [3]. We took into account $\mathcal{BR}(f_1(1285) \rightarrow \eta\pi^+\pi^-) = 0.35$, $\mathcal{BR}(\eta \rightarrow \pi^+\pi^-\pi^0) = 0.23$ (average values from PDG) to make estimates for the $pp\pi^+\pi^-\pi^+\pi^-\pi^0$ final state.

First, we discuss the 5-pion background with all components (1), (2), (3) listed in Table I. Figure 3a) shows the reconstructed invariant mass of $\pi^+\pi^-\pi^0$ with a clear signal of η meson ($m_\eta \approx 548$ MeV, $\Gamma_\eta \approx 1.31$ keV) on top of a large background. For the continuum background we take $\sigma_{\text{back}}^{5\pi} = 88 \mu\text{b}$ [10] (this should be regarded rather as an upper limit). The narrow width of the η meson allows to impose an extra mass cut on $M_{\pi^+\pi^-\pi^0}$ and suppresses the background efficiently. This is shown in Fig. 3b). The expected signal (~ 4000 counts) and background distributions display projections for about 30 days of measurement. In addition, the contribution (1) can be eliminated by using the side-band subtraction method.

In Fig. 3c) we show separately the contributions (2) and (4), in the $\pi^+\pi^-\eta$ invariant mass, to proof feasibility of the $f_1(1285)$ measurement by HADES Collaboration at $\sqrt{s} = 3.46$ GeV. We can see that the nonreducible background contribution from double excitation of N^* resonances has a broader distribution than the f_1 signal and this allows for observation of $f_1(1285)$ resonance in this process.

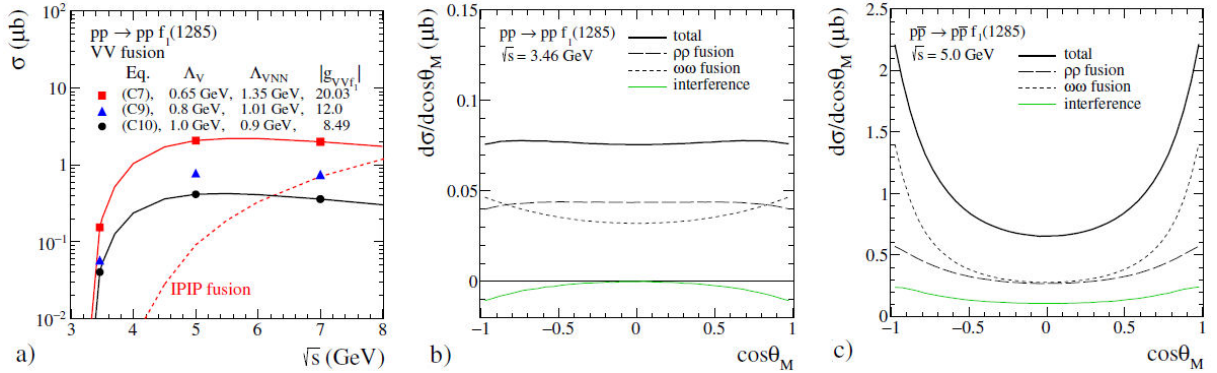


FIGURE 2. a) Cross section for the $pp \rightarrow pp f_1(1285)$ reaction as a function of collision energy \sqrt{s} for $VV \rightarrow f_1(1285)$ fusion mechanism for different parameters [3]; b) and c): Distributions in $\cos\theta_M$ for $\sqrt{s} = 3.46$ GeV and $\sqrt{s} = 5.0$ GeV, respectively. Results for the parameter values of (C7) are presented here. Shown are the contributions for the $\omega\omega$ - and $\rho\rho$ -fusion processes separately, their coherent sum (total), and the interference term (the green bottom solid line).

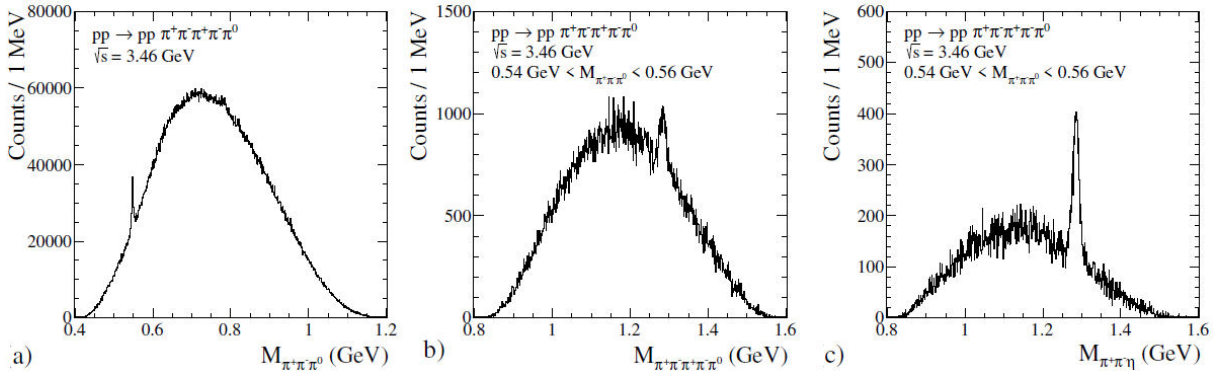


FIGURE 3. Invariant mass distributions of a) $\pi^+\pi^-\pi^0$, b) $\pi^+\pi^-\pi^+\pi^-\pi^0$, c) $\pi^+\pi^-\eta$ corresponding to the measurement of $pp \rightarrow pp\pi^+\pi^-\pi^+\pi^-\pi^0$ reaction at $\sqrt{s} = 3.46$ GeV with the HADES apparatus [3]. Contributions listed in Table I were included in the simulations (see the main text). The results in panels b) and c) include the cut on the η meson mass $0.54 \text{ GeV} < M_{\pi^+\pi^-\pi^0} < 0.56 \text{ GeV}$.

TABLE I. Contributions used in the simulations of the $pp \rightarrow pp\pi^+\pi^-\pi^+\pi^-\pi^0$ reaction.

Contribution	Cross section (μb)	Discussion
(1) $pp \rightarrow pp\pi^+\pi^-\pi^+\pi^-\pi^0$	88	$\sigma = (88 \pm 14) \mu\text{b}$ [10], $P = 5.5 \text{ GeV}/c$
(2) $pp \rightarrow pp\pi^+\pi^-\eta(\rightarrow \pi^+\pi^-\pi^0)$	0.18	Estimates via two N^* resonances, see Eqs. (4.4) and (4.5) of [3]
(3) $pp \rightarrow pp\pi^+\pi^-\omega(\rightarrow \pi^+\pi^-\pi^0)$	0.07	$\sigma = (0.09 \pm 0.03) \mu\text{b}$ [11] for $pp \rightarrow pp\pi^+\pi^-\omega$ at $P = 6.92 \text{ GeV}/c$
(4) $pp \rightarrow pp f_1[\rightarrow \pi^+\pi^-\eta(\rightarrow \pi^+\pi^-\pi^0)]$	0.012	$\sigma = (3.2 - 12.4) \text{ nb}$, see (3.1) and (3.3) of [3]

4. Conclusions

We have discussed the possibility to observe the $f_1(1285)$ meson in the $pp \rightarrow pp f_1(1285)$ and $p\bar{p} \rightarrow p\bar{p} f_1(1285)$ reactions at energies close to the threshold. The $\rho\rho$ and $\omega\omega$ fusion amplitudes have been used to estimate the total and differential cross sections for the HADES and PANDA experiments. Both processes play roughly similar role. The distributions in t (not shown here) and the distributions in $\cos\theta_M$ (Fig. 2) seem particularly interesting. The shape of these distributions gives information on the role of the individual fusion processes. We predict a large cross section for the exclusive $f_1(1285)$ production for the PANDA energy range. For the $VV \rightarrow f_1(1285)$ processes for $\sqrt{s} = 5.0 \text{ GeV}$ (PANDA) we have obtained about 10 times larger cross sections than for $\sqrt{s} = 3.46 \text{ GeV}$ (HADES).

We have discussed the possibility of a measurement of the $pp \rightarrow pp f_1(1285)$ reaction by the HADES Collaboration at GSI. With our estimate of the cross section for the $pp \rightarrow pp f_1(1285)$ reaction we expect that the $f_1(1285)$ could

be observed in the $\pi^+\pi^-\eta(\rightarrow \pi^+\pi^-\pi^0)$ channel since the η has a very small width and a cut on the η mass will reduce the background efficiently. We have performed feasibility studies and estimated that a 30-days measurement with HADES should allow to identify the $f_1(1285)$ resonance in the $pp\pi^+\pi^-\eta$ final state. From the $pp \rightarrow pp\pi^+\pi^-\pi^+\pi^-$ reaction it may be difficult to extract the $f_1(1285)$ signal due to large background contributions, for instance, from the double excitation of the $N(1440)$ resonances via the σ -meson exchange as previously noted in Ref. [3].

Acknowledgments

The author is indebted to A. Szczurek, O. Nachtmann, and P. Salabura for collaboration on related topics and discussions. Thanks to the organisers of the HADRON 2021 conference for making this presentation of our results possible. Presented in “19th International Conference on Hadron Spectroscopy and Structure in memoriam Simon Eidelman”, July 26-31, 2021, Mexico City (Mexico).

1. G. Agakishiev *et al.* (HADES Collaboration), The high-acceptance dielectron spectrometer HADES, *Eur. Phys. J. A* **41** (2009) 243,
2. G. Barucca *et al.* (PANDA Collaboration), PANDA Phase One, *Eur. Phys. J. A* **57** (2021) 6
3. P. Lebedowicz, O. Nachtmann, P. Salabura and A. Szczurek, Exclusive $f_1(1285)$ meson production for energy ranges available at the GSI-FAIR with HADES and PANDA, *Phys. Rev. D* **104** (2021) 034031
4. P. Lebedowicz, J. Leutgeb, O. Nachtmann, A. Rebhan, and A. Szczurek, Central exclusive diffractive production of axial-vector $f_1(1285)$ and $f_1(1420)$ mesons in proton-proton collisions, *Phys. Rev. D* **102** (2020) 114003
5. R. Sikora, *Measurement of the diffractive central exclusive production in the STAR experiment at RHIC and the ATLAS experiment at LHC*, PhD Thesis, AGH-UST, Cracow, 2020, CERN-THESIS-2020-235
6. C. Ewerz, M. Maniatis, O. Nachtmann, A Model for Soft High-Energy Scattering: Tensor Pomeron and Vector Odderon, *Annals Phys.* **342** (2014) 31, <https://doi.org/10.1016/j.aop.2013.12.001>
7. P. Lebedowicz, O. Nachtmann, A. Szczurek, Exclusive central diffractive production of scalar and pseudoscalar mesons; tensorial vs. vectorial pomeron, *Annals Phys.* **344** (2014) 301, <https://doi.org/10.1016/j.aop.2014.02.021>
8. R. Dickson *et al.*, (CLAS Collaboration), Photoproduction of the $f_1(1285)$ meson, *Phys. Rev. C* **93** (2016) 065202,
9. I. Fröhlich *et al.*, A Monte Carlo Simulation Tool for Hadronic Physics, *PoS ACAT* (2007) 076
10. G. Alexander *et al.*, Proton-Proton Interactions at 5.5 GeV/c, *Phys. Rev.* **154** (1967) 1284
11. S. Danieli *et al.*, Four- and five-pion production in pp collisions at 6.92 GeV/c, *Nucl. Phys. B* **27** (1971) 157